



**HAL**  
open science

## Biomechanical modelling of the foot

A Perrier, V. Luboz, M. Bucki, F Cannard, N. Vuillerme, Yohan Payan

► **To cite this version:**

A Perrier, V. Luboz, M. Bucki, F Cannard, N. Vuillerme, et al.. Biomechanical modelling of the foot. Y. Payan and J. Ohayon. Biomechanics of Living Organs: Hyperelastic Constitutive Laws for Finite Element Modeling, Elsevier, pp.545-563, 2017, 9780128040096. 10.1016/B978-0-12-804009-6.00025-0 . hal-01930207

**HAL Id: hal-01930207**

**<https://hal.science/hal-01930207>**

Submitted on 21 Nov 2018

**HAL** is a multi-disciplinary open access archive for the deposit and dissemination of scientific research documents, whether they are published or not. The documents may come from teaching and research institutions in France or abroad, or from public or private research centers.

L'archive ouverte pluridisciplinaire **HAL**, est destinée au dépôt et à la diffusion de documents scientifiques de niveau recherche, publiés ou non, émanant des établissements d'enseignement et de recherche français ou étrangers, des laboratoires publics ou privés.

## Chapter 18: Biomechanical modelling of the foot

A. Perrier<sup>1,2,3</sup>, V. Luboz<sup>2</sup>, M. Bucki<sup>2</sup>, F. Cannard<sup>2</sup>, N. Vuillerme<sup>3,4</sup> & Y. Payan<sup>1</sup>

1 Univ. Grenoble Alpes & CNRS, TIMC-IMAG, F-38000 Grenoble, France, {antoine.perrier, yohan.payan}@imag.fr;

2 TexiSense, Montceau-les-Mines, France, {antoine.perrier, vincent.luboz, marek.bucki, francis.cannard}@texisense.com;

3 Univ. Grenoble Alpes, AGEIS, F-38041, Grenoble, France, Nicolas.Vuillerme@agim.eu

4 Institut Universitaire de France, Paris, France

**Abstract:** The foot is a key structure during gait as it adapts to the ground geometry to insure balance and it stores energy to ease the next step. Because this functionality can be affected, by morphological issues or by aging or disease like diabetes, modelling the foot could help in understanding its correct behavior and the way to avoid or solve pathological behaviors. In this chapter, after presenting the foot anatomy and functionality, we propose a summary of the main foot models published in the literature. We also introduce our biomechanical model, using a Finite element mesh representing several soft tissue layers surrounding rigid bones and cables simulating the ligaments. Two clinical applications, namely ankle arthrodesis and foot ulcer prevention, are also presented.

**Keywords:** foot model, biomechanical analysis, heterogeneous soft tissues, clinical applications

### 1. Introduction: clinical context

Understanding the foot anatomy is essential to analyze its functionalities, its pathologies, and the way they can be prevented and treated with orthosis or surgery for instance. These complementary fields of research have yielded to several significant breakthroughs helping understanding the foot, using models adapted to each clinical applications. The first field concerns the physiology of the foot and more especially the way the foot behaves in conjunction with other structures (for example the leg or the ground) and their modifications to monitor the adaptation of the foot to various conditions. Furthermore, among the different clinical fields, we can mention three other fields studying the foot on the pathological side: diabetes, orthosis, and surgery. Diabetes is a pathology affecting the foot through a lack of sensitivity due to the neuropathy it implies (Mueller, 1992). As a consequence, diabetic patients have trouble feeling pain in their foot and can consequently undergo pressure ulcer due to high tissue deformations (because of ischemia or cell destruction). Furthermore, diabetes can create joint lesions because of the neuropathy. The third field of research to understand the foot is devoted to orthoses. It concerns studies investigating the influence of a device on the pressure load around the foot, the geometrical changes applied on the bones, or the behavior of the foot after an impact (Lemmon et al., 1997). The orthosis influence is analyzed based on its shape and/or the materials it uses. Finally, the fourth field of research aims at improving foot surgeries. It concerns mainly the understanding of a surgical gesture, and the influence of an action on the foot structure and functions. It can also investigate the coupling between a foot joint and prosthesis.

### 2. Anatomical description of the foot

The foot anatomy being complex, it is essential to comprehend it before moving to one of the four fields mentioned above. The human foot is composed of 28 bones and 33 joints (including five main joint complexes: the ankle, the subtalar joint, the tarsal transverse joint, the tarso-metatarsal joint, and the metatarsophalangeal joint). Several bone regionalization schemes have been proposed, one of the most popular is described in figure 18.1 and divides the foot in four regions: the back foot (talus and calcaneus), the medio foot (cuboid, navicular, and the three cuneiform bones), the metatarsus (from M1 to M5), and the toes (from hallux to quintus). The foot has three extrinsic muscle regions located on the tibia and fibula: the anterior region (with the tibial anterior, the hallux long extensor, and the toes' long extensor muscles), the lateral region (with the long fibula and the short fibula muscles), and the posterior region (with the tibial posterior, the hallux long flexor, the toe long flexor muscles, and the sural triceps). Four muscle regions are intrinsic: the dorsal region (with the short extensor

muscles of the hallux and of the toes), the medial region (with the abductor and adductor of the hallux, and the short flexor of the hallux), the lateral region (with the abductor of the quintus, the short flexor of the quintus, and the opposing muscle of the quintus), and the median region (with the short flexor of the toes, the plantar square, the interosseous dorsal muscles, the interosseous plantar muscles, and the lumbrical muscles). These muscles allow a wide range of foot motions: dorsiflexion, plantar flexion, pronation, supination, abduction, adduction, inversion and eversion.

FIGURE 18.1 HERE

The foot is a poly-articular system, surrounded by soft tissues, with several joint chains in parallel and serialized in the four previously described regions (figure 18.1). It is a key structure during gait as it adapts to the ground geometry to insure balance and it stores energy to ease the next step in a non-pathological configuration. The foot objective is to transmit the best force vector to the rest of the lower leg whatever the contact surface type (texture, form, rigidity...) or the aim of the gesture (gait, turn, jump, get up, run...). To achieve these goals, the foot must be able to adapt to the shape of the ground, to rigidify itself (good transmission of the vector fields from the lower leg or the external forces), to be thrifty for an optimized gesture (long walk, swim, running...).

The serialized organization of the foot allows force transmission from rear foot to front foot during the first contact of the foot on the ground, and then from front foot to rear foot during the digitigrade phase. The parallel chains are active in the rear to front axis and also in the medio lateral axis.

The plantar aponeurosis (or plantar fascia) is one of these soft tissues. It helps preventing the stretching of the foot structures. It can be stretched about 10 percent, and has extra length under each metatarsal head in connection with the first phalange of each toe. It has a joint action with the trans-metatarsal ligament to prevent lateral foot stretching, in conjunction with the interosseous muscles. Other ligaments link each bone with its neighbors to create the joints using a complex mechanism mixing bone contacts and cable like connections between ligaments. The poly-articular chain system allows the foot to modulate its length, width and height during loading. If for some reasons, the chains are rigid, the strains are propagated to the foot extremities instead of the center of the foot, which usually concentrates the constraints. The foot is also composed of fat tissue, mainly to serve as a cushion for the other structures. In particular, below the calcaneus, the fat pad is composed of several nodules of high density fat to compensate the impact of the whole body below the heel at the first contact with the ground. Finally, the foot soft tissues are embedded within the protective skin layer.

Most of the gait theory is based on conclusions considering only the bones (position and contacts). To the best of our knowledge, soft tissues have not been integrated in early works. However, to be useful and usable in clinical practice, a foot model therefore needs to integrate this component.

### 3. Foot models in the literature

Several reviews have already summarized a list of foot models over the past few years. Among them, that recently published by (Telfer et al., 2014) provides a comprehensive review on diabetic foot modelling and investigates several aspects such as the bone geometry, the internal constraints, the soft tissue material properties, the skin surface pressures and their spreading, and the interactions between the foot and the device around the foot. Another review, from (Wang et al., 2016), focuses on the shoe and the insole and aims at designing the most adapted device for a given foot. Recently, Perrier (2016) further draws a complete survey of most of the foot models presented in the literature, table 18.1. We propose to summarize this review below with few key articles.

TABLE 18.1 HERE

The first biomechanical model was a 2D model introduced by Lemmon and Cavanagh (Lemmon et al., 1997). Using baropodometry analyzing the plantar pressures, these authors validated their model results against clinical measurements. This work stemmed research studies in the field of diabetes and orthopedic surgery and is still a reference in terms of validation. It showed that insole thickness has an influence on pressure peaks under metatarsal heads. It used a linear constitutive law to model the bone material with a Young's modulus of 10 GPa and a Poisson's ratio of 0.34. A Mooney-Rivlin constitutive law was used to model the soft tissues as a hyper-elastic material. In vivo load-deformation data were collected on five subjects using an ultrasound device in conjunction with a load cell. It lead to a simplified Finite Element model with coefficient values of  $C_{10} = 85,550 \text{ N.m}^{-2}$ ,  $C_{01} = -58,400 \text{ N.m}^{-2}$ ,  $C_{20} = 38,920 \text{ N.m}^{-2}$ ,  $C_{11} = -23,100 \text{ N.m}^{-2}$ ,  $C_{02} = 8,484 \text{ N.m}^{-2}$ ,  $D_1 = 0.4370\text{E}05 \text{ N.m}^{-2}$ ,  $D_2 = 0.6811\text{E}-06 \text{ N.m}^{-2}$ .

Another 2D model was introduced by (Gefen, 2000) and validated on six phases of gait, using plantar pressure measurements, in a quasi-static set up. This article stemmed foot functional analysis based on biomechanical models. It was followed in (Gefen, 2003) by a more complete model demonstrating that pressures measured at

skin surface lead to a strain increase in deep tissues. From this conclusion, it was hypothesized that pressure ulcers may originate deep in the tissues and not only at the foot surface. In this article, the bones and cartilages were modelled as linear, elastic and isotropic materials, while ligaments, fascia and the soft tissue fat pad were considered as being non-linear materials using an Ogden constitutive law. Young's modulus and Poisson ratio for bone were taken as being 7,300 MPa and 0.3, respectively, and for cartilage as 10 MPa and 0.4, respectively. The Poisson ratios were taken as 0.4 for the ligaments and fascia and 0.49 for the soft tissue pad. The elastic properties of these soft tissues were derived from stress-strain data published by (Nakamura et al., 1981) but were not given in the article.

One of the first 3D biomechanical models was introduced by (Chen et al., 2003) and showed that an orthosis with an optimal contact with the foot decreases the skin surface pressures and spread them more evenly below the foot. From this conclusion, it seems that a pressure ulcer may appear on a foot depending on the pressure field applied on its surface. Using a 3D Finite Element model therefore appears to be appropriate to estimate the consequences of various orthoses on the foot. In this paper, the foot bone and soft tissue were assumed to be linear, elastic solids. Their Young's moduli and Poisson ratio were respectively 10 GPa and 0.34 for the bones, 1.15 MPa and 0.49 for the soft tissues, and 10 MPa and 0.4 for the cartilage. Five cables were used to model the plantar aponeurosis and three cables for the short plantar ligaments. Their stiffness was 11.5 MPa. An improvement of this 3D model was presented in (Chen et al., 2010), with the integration of active muscles, almost all foot ligaments, and soft tissues modelled with the Mooney Rivlin constitutive law defined in (Lemmon et al., 1997) with the same parameters. It showed that internal strains and pressures below the metatarsal heads are directly influenced by the force given by the triceps.

Another 3D model has been proposed by (Cheung et al., 2005). It showed that (1) the shape of an orthosis is more important than its materials when it comes to strain distribution and (2) a higher soft tissue stiffness implies higher skin surface pressures. Bones and the soft tissues were also represented as Finite Element models. Except for the soft tissue, all other tissues were idealized as homogeneous, isotropic and linearly elastic materials. The Young's modulus and Poisson's ratio for the bony structures, the cartilage, ligaments, and plantar fascia were selected from the literature (Gefen, 2000). The soft tissue properties of the whole foot were also inspired by the heel pad properties given in (Lemmon et al., 1997) as a nonlinearly elastic material represented by a Mooney-Rivlin constitutive law. This model was used by (Wong et al., 2015) for clinical applications in orthopedic surgery and more specifically in the arthrodesis of the first tarso-metatarsal joint and its consequence on gait.

Although the models presented above tend to integrate complex structures and allow studying various clinical fields, they still miss some of the anatomy of the foot (especially no model represents the foot material heterogeneity as the foot is composed of different layers of soft tissues: skin, fat, muscles), they are not patient specific (as they are all modelled from one patient's data, or from an idealized morphology), and they cannot be used clinically as they require long computations (more than one hour). The main limitation concerns the realism of the model: it must be accurate if useful results are needed and therefore the model should not simplify the morphology of the patient and the way the mechanical properties are estimated. A nonlinear heterogeneous model, i.e. with several layers of soft tissues to represent the skin, fat and muscles, consequently seems to be important to simulate the foot accurately. Nevertheless, the key aspect of a good biomechanical model is that it should be adapted to the function (gait, balance, pressure distribution...) it wants to simulate, using an appropriate mechanical hypothesis and an appropriate level of details for the morphology.

#### **4. Biomechanical foot model for arthrodesis simulation and foot pressure ulcer prevention**

In an attempt to improve the previous foot models in a more realistic manner and with an impact on several applications, we have proposed to generate a detailed biomechanical model to study arthrodesis and foot pressure ulcer prevention.

A series of medical image acquisitions has been performed on a healthy volunteer (no trauma, surgery or specific pathology of the foot) to obtain morphological data and create his biomechanical foot model. Two imaging modalities were used for this individual (31 years old, 173cm, 84 kg): a CT scan with slices every 0.6 mm, and an MRI scan with slices every 5mm. The scans were segmented to extract the 3D surfaces of the various foot structures: 28 separated foot bones, tibia and fibula, and four layers of soft tissues, namely the skin, the heel fat pad, the fat for the rest of the foot, and the muscles. To allow fast enough computation time, we chose to represent the bones as rigid bodies to concentrate on the cinematic of those structures, especially before and after arthrodesis. On the other hand, since we want to measure the strains inside the soft tissues, in order to study foot pressure ulcer, the soft tissues have been modelled as a Finite Element mesh. Rigid bodies and Finite Element mesh have been coupled semi implicitly in the ArtiSynth open source framework (Lloyd et al., 2012).

To be realistic in physiological and dynamic points of view, the mass of the different structures have been estimated from (De Leva, 1996), with a foot mass of 1.37 % of the subject mass. A density of  $1850 \text{ kg.m}^{-3}$  was

set for the bones, leading to a whole bony mass of 0.443 Kg. The density of the soft tissues was set to  $1\,200\text{ kg}\cdot\text{m}^{-3}$  to reach a soft tissue mass of 1.13 Kg.

The muscle and ligament insertions were defined from the medical imaging data and from the literature, Figure 18.2. Cables were used to model the 210 ligaments of the foot included in our model. These cables constrain the elongation of the structures with a linear elongation stiffness of 395 MPa while the structures are free to move towards each other since the compression stiffness is set to 0 MPa. Furthermore, to simulate the coaptation of the bones, the rest length of the cables was set to 90 % of the initial length of the model since the foot was acquired while the subject was lying down with an initial length that is not representative of the position of the bones when standing. Overall, the joints are modelled as the contacts between the bones and are constrained by the ligaments. Plantar aponeurosis is also simulated in our model. It is composed of five cables connecting the calcaneus to each toe first phalange. Transversal cable connections constrain the aponeurosis in the three directions.

FIGURE 18.2 HERE

Fifteen extrinsic and intrinsic muscles are integrated in our foot model. They are simulated as cables using a Hill constitutive law. Their path has been determined on the MRI scan. Each muscle can be activated independently, i.e. its length can be shortened simulating muscle contraction. Since the foot is relaxed during the MRI acquisition with the patient lying down, its muscles are not contracted. Muscle length at equilibrium during stance had therefore to be defined as a ratio of these muscles' MRI lengths. This was defined manually for each muscle and led to length ratios between 0.73 and 0.91. The maximum force developed by a muscle was set by computing the displacement of half the body weight when the foot is in charge. For example, to raise the heel by contracting the two bi articular muscles of the triceps, a force of 1,800 N is needed. This value corroborates the 1,620 N given in (Chen et al., 2010) in a quasi-static setup.

The soft tissue Finite Element mesh was generated by a software from Taxisense company and based on (Lobos et al., 2010). It uses the surfaces segmented from the CT scan to define the different domains in the foot and to generate the continuum. This meshing algorithm tends to maximize the number of hexahedrons in the generated mesh to avoid the locking mechanism linked to tetrahedrons in quasi incompressible materials. The final mesh is composed of 142,060 elements (18,784 hexahedrons, 38,774 wedges, 56,655 tetrahedrons, and 27,847 prisms) with a discretization of 3 mm. It is composed of four domains: the skin, the heel fat pad, the rest of the fat, and the muscles, Figure 18.3. The bones are modelled as rigid bodies and no Finite Elements are included in them.

FIGURE 18.3 HERE

To achieve a nonlinear hyper-elastic behavior, a Neo Hookean constitutive law is used in the Finite Element model, defined by a strain energy density function  $W$  such as:

$$W=C_{10}(I_1-3)+(J-1)^2/D$$

Where  $I_1$  is the first invariant of the left Cauchy-Green deformation tensor,  $C_{10}$  is a material parameter,  $J$  is the determinant of the deformation gradient  $F$  and  $D$  is a material incompressibility parameter. The Neo Hookean model was chosen because of its simplicity to apprehend its parameters. It indeed uses only two material parameters that can be compared to known material parameters, with  $D$  linked to the Poisson ratio  $\nu$  [ $D=(1-2\nu)/C_{10}$ ] and  $C_{10}$  that can provide an estimation of the equivalent Young's modulus  $E$  at small strains [ $E\approx 6* C_{10}$ ]. Furthermore, Neo Hookean models are good representations of the reality in compression, or at least similar to Mooney Rivlin materials, with fewer parameters and more stability. In addition, since the foot is mainly submitted to compression, this range of deformations is well modelled using a Neo Hookean constitutive law.

Each soft tissue layer (or domain) has its own material parameters to simulate different behaviors and derives from earlier work (Luboz et al., 2015). It leads to the following four material properties:

- For the skin, a Young's modulus of 200 kPa and a Poisson ration of 0.485,
- For the heel fat pad, a Young's modulus of 100 kPa and a Poisson ration of 0.499,
- For the rest of the fat,, a Young's modulus of 30 kPa and a Poisson ration of 0.49,
- For the muscles, a Young's modulus of 60 kPa and a Poisson ration of 0.495.

This model was used for two different applications: ankle arthrodesis and pressure ulcer prevention.

The first one consisted in investigating ankle mobility during muscle contraction with and without arthrodesis. Dorsal and plantar flexions of the ankle were simulated by activating the foot muscles of our model while assessing the mobility of the talus bone and the foot. Dorsal flexion activation is performed in three movements: (1) activation of the toe and hallux extensor muscles alone, (2) contraction of the tibialis anterior muscle alone, and (3) combined contraction of the extensors and the tibialis anterior muscles. Plantar flexion activation is divided into four movements: (1) activation of toes and hallux flexor muscles alone, (2) contraction of the tibialis posterior muscle alone, (3) contraction of the triceps, and (4) combined contraction of all those ankle flexor

muscles. During those movements, the 3D angle formed by the tibia center, the talus center, and the second metatarsal head center gives an estimation of the foot opening angle. The simulated arthrodesis set the angle between the tibia and talus to  $117^\circ$ ; it therefore limits the foot opening angle. This angle range of motion is accepted to be for healthy subjects between  $60^\circ$  and  $80^\circ$ . The goal of this study was to estimate the arthrodesis influence by comparing the foot opening angle with and without arthrodesis.

FIGURE 18.4 HERE

The second simulation consisted in investigating pressure ulcer risk in the foot and improving prevention. Foot pressure ulcers are a common complication of diabetes because of patient's lack of sensitivity due to neuropathy. They mainly result from excessive skin surface pressure intensity (leading to internal strains above 50 % for about 10 minutes) or prolonged compression (leading to internal strains above 20 % for about two hours) (Loerakker et al., 2011). Monitoring the internal strains using a biomechanical model combined with skin surface pressure measurements could consequently improve the estimation of pressure ulcer risk and help patient daily prevention. We therefore used our biomechanical foot model to simulate a pressure load applied below the foot during static unipodal stance. The plantar pressure pattern was measured using a commercially available pressure sensor (Zebris platform, <http://www.zebris.de/>) under the right foot of the subject used to build our model. The maximal pressure appears below the calcaneus with a peak value of  $14.5 \text{ N.cm}^{-2}$ . During the simulations, the tibia was fixed while the fibula and the foot were free. The simulation is divided in two phases: (1) reaching equilibrium of the foot while tendons, ligaments and muscles of the model tend to recover their optimal length (defined by the ratio of their initial length) and thus generate pre-stresses in the FE continuum, and (2) gradual application of the pressure pattern below the foot. Once the full pressure is applied and equilibrium is reached, peak internal Von Mises strains have been recorded as well as the cluster volumes of soft tissues above the 20 % and 50 % strain thresholds and defining the risk of pressure ulcers. A cluster is defined as the contiguous elements having a strain peak above one of those two thresholds (Bucki et al., 2016). The aim of this study was to estimate the amount of tissues at risk in this configuration and to determine if our model could help in pressure ulcer prevention.

## 5. Results and discussions

### 5.1 Arthrodesis simulation

The simulation of the ankle arthrodesis allows to explore the relationships between adjacent joints and to quantify their respective amplitudes within a foot motion. The combined action of the anterior muscles induces a maximal dorsal flexion of  $42^\circ$  for the foot opening angle without arthrodesis while this angle is limited to  $9^\circ$  with arthrodesis. The combined action of the posterior muscles induces a maximal plantar flexion of  $33^\circ$  for the foot opening angle without arthrodesis while this angle is limited to  $14^\circ$  with arthrodesis.

Moreover, it is possible to analyse the amplitude of motion for other joints and to estimate their influence during arthrodesis. For example, the angle between the navicular and the talus projected on the sagittal plane during dorsal flexion has a value of  $3^\circ$ . This rotation is produced by the navicular alone since the talus is fixed. Furthermore, the dorsal flexion being  $9^\circ$ , the remaining  $6^\circ$  are probably provided through the Cuneo-metatarsal and Cuneo-navicular joints which are mobilized by the synergistic contraction of the anterior muscles. A similar analysis can be performed for the plantar flexion, leading to an estimation of the muscles' influence.

Based on this example, a biomechanical foot model, driven by muscle activations reproducing the swing motion of the foot with and without arthrodesis, could be used for arthrodesis planning to find the optimal setting of the foot opening angle in order to optimize swing phase during gait. Naturally, the results above need to be validated on real cases before moving to surgical planning. To this aim, a patient specific process to generate a numerical clone of the patient foot would be needed. Using the method presented in (Bucki et al., 2016) will help to reach this goal. This method is based on the registration of each patient's skin and bone surfaces (extracted from a medical image dataset) with the surfaces of an atlas model. The registration is divided into three steps: rigid registration, affine registration, and local elastic registration. It avoids the tedious and time consuming generation of a new patient mesh and takes few minutes to create a numerical clone for each patient. It consequently gives the possibility to create new patient models easily and to help in surgery planning.

### 5.2 Pressure ulcer prevention

The simulation of static unipodal stance allows estimating the impact of a pressure pattern below the foot and inside the soft tissues. For example, for our model, the highest cluster volume is located in the heel region with  $50.8 \text{ cm}^3$  with Von Mises strains above 20 %. No cluster has a volume higher than  $0.2 \text{ cm}^3$  when a threshold of 50 % is considered. This almost negligible value seems normal since the pressure applied below the foot is not

supposed to cause short term pressure ulcer as it is a unipodal stance. Analyzing only the peak Von Mises strains, figure 18.5, is not really representative as the highest value is in the toe region (161 %), but the cluster volume around this peak strains is extremely small (less than 0.01 cm<sup>3</sup>). This peak pressure is probably due to a numerical singularity because of a highly deformed element and not really representing the internal strain in this region. Using the cluster volume is consequently more representative as it bypasses those numerical singularities. Overall, the estimation of the cluster volume in our biomechanical model allows determining the level of deformation in the foot when a pressure load is applied below it. It could therefore be used to determine the risk of pressure ulcer and to complete efficiently the monitoring of the skin surface pressure.

FIGURE 18.5 HERE

Nevertheless, to allow daily prevention, a model should be fast enough to compute a simulation interactively and it should be coupled to a sensor usable during daily tasks. The computation time of a simulation is difficult to reduce since a high level of details is needed to achieve realistic simulations. The principal area of research here is in the pre computation of most of the possible scenarios to use them as a library on which a daily analysis is based to determine if a specific case, interpolated from the library, produces internal strains high enough to lead to pressure ulcer. Model reduction (Cueto et al., 2014) could also be implemented to speed up the computation. Although fairly inaccurate when the given pressure scenario is outside of the library range, it is accurate and fast when the library covers a wide enough range of scenarios. In term of pressure sensors usable on a daily basis, several are commercially available (such as the ones proposed by Novel, Tekscan, Vista Medical or Taxisense). The key here is to be wearable in a shoe, as an insole or a sock, and to send pressure pattern information regularly to feed simulations with pressure patterns. Finally, for a patient specific prevention, a numerical clone of the patient is needed as the morphology of the patient has a clear impact on the risk of pressure ulcer as demonstrated by (Luboz et al., 2015). Again, using the method presented in (Bucki et al., 2016) could help to reach this goal.

## 5. Conclusion

The foot is a complex structure, involving 28 bones, 30 joints, 210 ligaments, and several layers of soft tissues (skin, fat, muscles). Its purposes are to adapt to the ground during gait or stance, and to store and use the energy while walking. Understanding its behavior during non-pathological function is a whole field of research. Furthermore, it can be afflicted by various pathologies (such as diabetes) or abnormalities (such as hallux valgus), leading to the use of specific devices (orthosis, prosthesis), or even surgery. Musculoskeletal and biomechanical models have been introduced to help understanding these various fields. These models use more or less complex representations, from purely geometrical to biomechanical models using Finite Element modelling to translate constitutive laws that can be linear elastic or more complex nonlinear hyper-elastic and they can model the foot as homogeneous or represent its heterogeneity and the different layer of soft tissues. Given the complexity of the foot, and the variety of behaviors of its components (especially the soft tissues), an accurate model requires a detailed representation of each constituents. This leads to at least two disadvantages: 1) creating a precise foot model is a tedious and long task, and 2) the computation time of a simulation with such model can be very long (quantified in hours). Most of the models published in the literature are either presenting a generic model (with an average ideal morphology) or a clone of a specific patient, therefore creating only one model and avoiding the repetitiveness of the task for other patients. A solution to build rapidly new numerical clones would be to use a registration technique aiming to adapt an atlas model to the morphology of each new patient, in the same fashion as in (Bucki et al., 2016). As for the computation time, simulations are most of the time performed for a specific application, and not repeated through a daily clinical set up. It is consequently not a problem to run several simulations over a long period and have the results to be analyzed later. If these models are needed in daily clinical investigations, with a need of interactions, a solution would be to precompute a set of simulations representing a wide range of scenarios and use them to interpolate the results from this abacus.

## Acknowledgements

Competing interests: Some authors are involved with the TexiSense Company ([http://www.taxisense.com/home\\_en](http://www.taxisense.com/home_en)).

Funding: This work was partly funded by the 2010 ANR TecSan IDS project, by the CAMI Labex (ANR-11-LABX-0004) and by the Institut Universitaire de France.

Ethical approval: the study was approved by the French institutional review board of Grenoble (IRB 5891 (CECIC) for Rhône-Alpes-Auvergne).

## References

1. Bucki M., Luboz V., Perrier A., Champion E., Diot B., Vuillerme N., Payan Y. Clinical workflow for personalized foot pressure ulcer prevention. *Medical Engineering & Physics*, 2016, DOI: 10.1016/j.medengphy.2016.04.017.
2. Chen W.P., Ju C.W., Tang F.T., Effects of total contact insoles on the plantar stress redistribution: a finite element analysis. *Clinical Biomechanics* 18, 17–24, 2003.
3. Cueto E. & Chinesta F. Real time simulation for computational surgery: a review. *Advanced Modeling and Simulation in Engineering Sciences*. 1:11, 2014.
4. De Leva P. Adjustments to Zatsiorsky-Seluyanov's segment inertia parameters. *Journal of Biomechanics*. 29(9):1223-30, 1996.
5. Gefen A., Megido-Ravid M., Azariah M., Itzhak Y., Arcan M. Integration of plantar soft tissue stiffness measurements in routine MRI of the diabetic foot. *Clin Biomech*. 16:921–5, 2001.
6. Gefen A. Plantar soft tissue loading under the medial metatarsals in the standing diabetic foot, *Medical Engineering & Physics* ; 25:491–499, 2003.
7. Lemmon D., Shiang T.Y., Hashmi A., Ulbrecht J.S., Cavanagh P.R. The effect of insoles in therapeutic footwear—a FE approach. *Journal of Biomechanics*, 1; 30(6):615–20, 1997.
8. Lloyd J.E., Stavness I. & Fels S. ArtiSynth: a fast interactive biomechanical modeling toolkit combining multibody and finite element simulation. *Soft Tissue Biomechanical Modeling for Computer Assisted Surgery, Studies in Mechanobiology, Tissue Engineering and Biomaterials*, 11:355–394, 2012.
9. Lobos C., Payan Y, & Hitschfeld N. Techniques for the generation of 3D Finite Element Meshes of human organs. *Informatics in Oral Medicine: Advanced Techniques in Clinical and Diagnostic Tech*. Hershey, PA: Medical Information Science Reference, pp. 126-158, 2010.
10. Loerakker S., Manders E., Strijkers G.J., Nicolay K., Baaijens F.P.T., Bader D.L., et al. The effects of deformation, ischaemia and reperfusion on the development of muscle damage during prolonged loading. *Journal of Applied Physiology*;111(4): 1168-1177, 2011.
11. Luboz V., Perrier A., Bucki M., Diot B., Cannard F., Vuillerme N., & Payan Y. Influence of the Calcaneus Shape on the Risk of Posterior Heel Ulcer Using 3D Patient-Specific Biomechanical Modeling. *Annals of Biomedical Engineering*, 43(2): 325-335, 2015.
12. Mueller M.J. Etiology, evaluation, and treatment of the neuropathic foot. *Critical Reviews of Physical and Rehabilitation Medicine*. 3: 289–309, 1992.
13. Nakamura S., Crowninshield R.D., Cooper R.R. An Analysis of Soft Tissue Loading in the foot – a Preliminary Report. *Bulletin of Prosthetics Research, BPR 10-35*, 18:1, 27-34, 1981.
14. Perrier A. Conception et évaluation d'un modèle biomécanique, éléments finis, patient-spécifique, du pied humain - Applications en podologie, orthopédie et diabétologie. Thesis manuscript, 199 pages, Université Grenoble Alpes, 2016.
15. Telfer S., Erdemir A., Woodburn J., & Cavanagh P. R. What Has Finite Element Analysis Taught Us about Diabetic Foot Disease and Its Management ? A Systematic Review, *PLoS ONE*, 9(10), 2014.
16. Wang Y., Wong D.W.C., Zhang M. Computational Models of the Foot and Ankle for Pathomechanics and Clinical Applications: A Review. *Annals of Biomedical Engineering*, 44(1):213-21, 2016.
17. Wong D.W.C., Wang Y., Zhang M. Functional Restoration and Risk of Non-union of the First Metatarsocuneiform Arthrodesis for Hallux Valgus: A Finite Element Approach. *Journal of Biomechanics*. 18;48(12):3142-8, 2015.

Figure captions:

Figure 18.1: Transverse regionalization of the foot, with four regions: the back foot (talus and calcaneus), the medio foot (cuboid, navicular, and the three cuneiform bones), the metatarsus (from M1 to M5), and the toes (from hallux to quintus).

Figure 18.2: The musculoskeletal model with 30 bones, 15 activated muscles (in red) and 210 ligaments (in green). The insertions of those structures have been determined on the MRI scan and from the literature.

Figure 18.3: The complete biomechanical foot model with the bony structures as rigid bodies, and the soft tissues as a Finite Element mesh. The soft tissues are divided in four layers: the skin (in pink), the heel fat pad (in green), the rest of the fat (in yellow), and the muscles (in red).

Figure 18.4: Dorsiflexion under three different muscle activations: on the left, activation of the toe and hallux extensor muscles alone; on the center, contraction of the tibialis anterior muscle alone; and on the right, combined contraction of the extensors and the tibialis anterior muscles.

Figure 18.5: Peak Von Mises strains in the foot during unipodal stance pressure load. The blue area corresponds to a strain value close to 0 % while the red area is for the peak strain at 161 %. Left, with 20 % of the total pressure, the strains remain below the 20 % strain threshold. Right, with 100 % of the pressure load, the peak strain reaches 161 % (area in red in the toes). It can be seen that the cluster volume (contiguous elements with a color different than blue) is larger in the heel region.

Table captions:

Table 18.1: Survey of the foot models presented in the literature with: the first author of the reference, the team leader, the year of publication, the application, the constitutive law, and the material parameters. Lig = ligaments, SoftTis = Soft Tissues, Li = Linear material (all rows in blue in the table), NoLi = Non Linear material (all rows in yellow in the table) with a non-specified constitutive law, Og = Ogden material (all rows in orange in the table), MoRi = Mooney Rivlin material (all rows in green in the table), Neo Hook heterogeneous material (rows in red), El = Elastic material, HyEl = Hyper-elastic material, Ho = Homogeneous material, Is = Isotropic material.

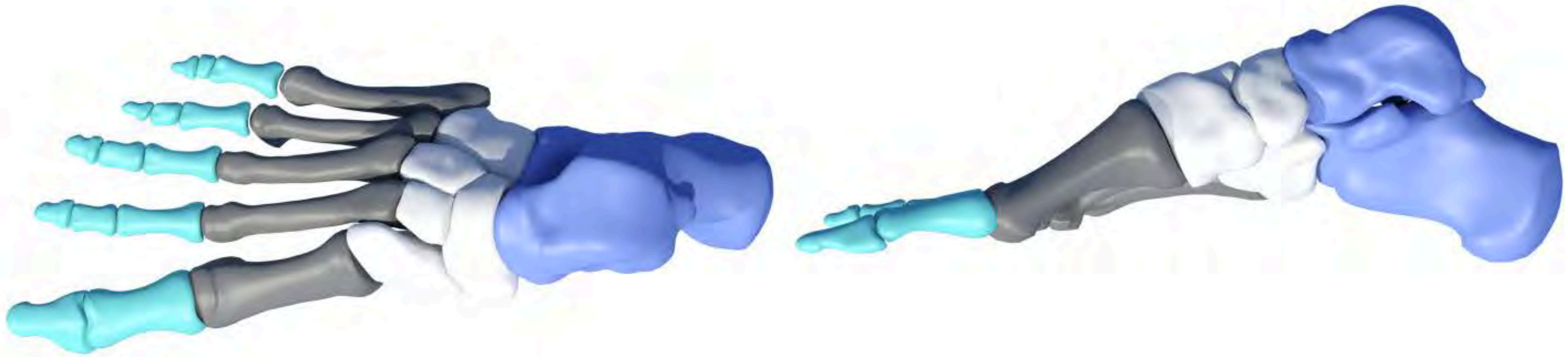
# Transversal regionalization

Hindfoot

Metatarsal bones

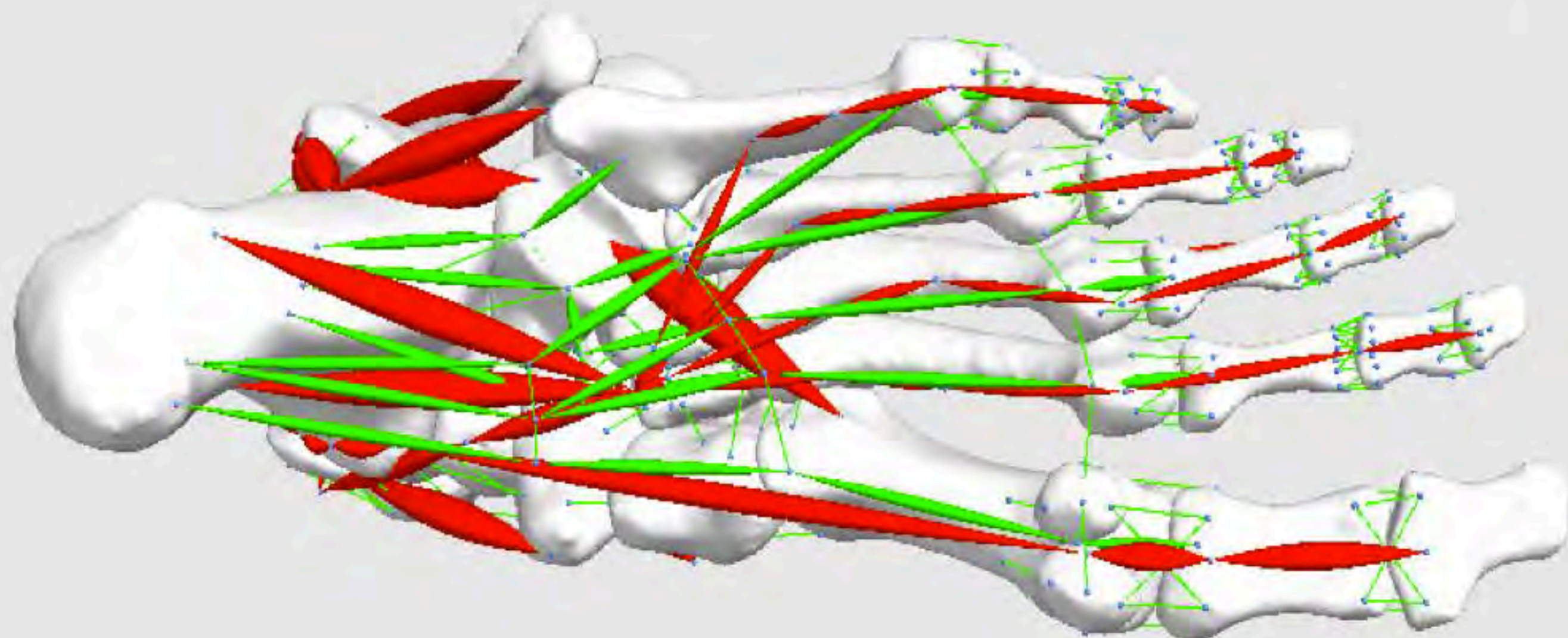
Midfoot

Toes



## Multibody rigid model

- 30 Bones (Rigid Bodies)
- 210 Ligaments (Cables)
- 15 activated muscles
- Plantar Aponeurosis ( 5 multi points cables with transverse connections)
- Joints modelled by the coupling of bone contacts, ligaments and muscles



- Ligaments
- Muscles

Bone density : 1850kg/m<sup>3</sup>

Skeleton mass : 0.443 Kg



Bones



Skin



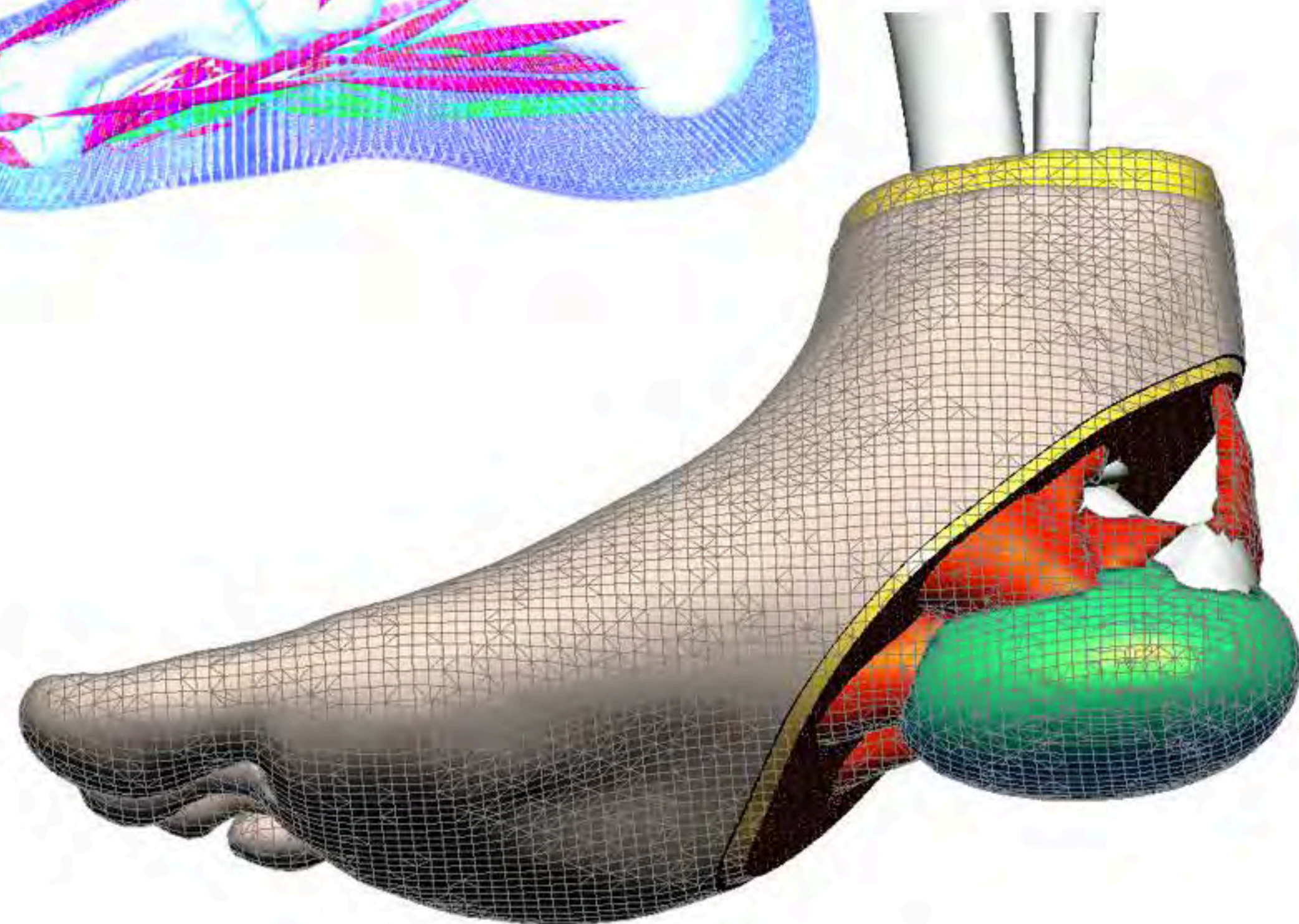
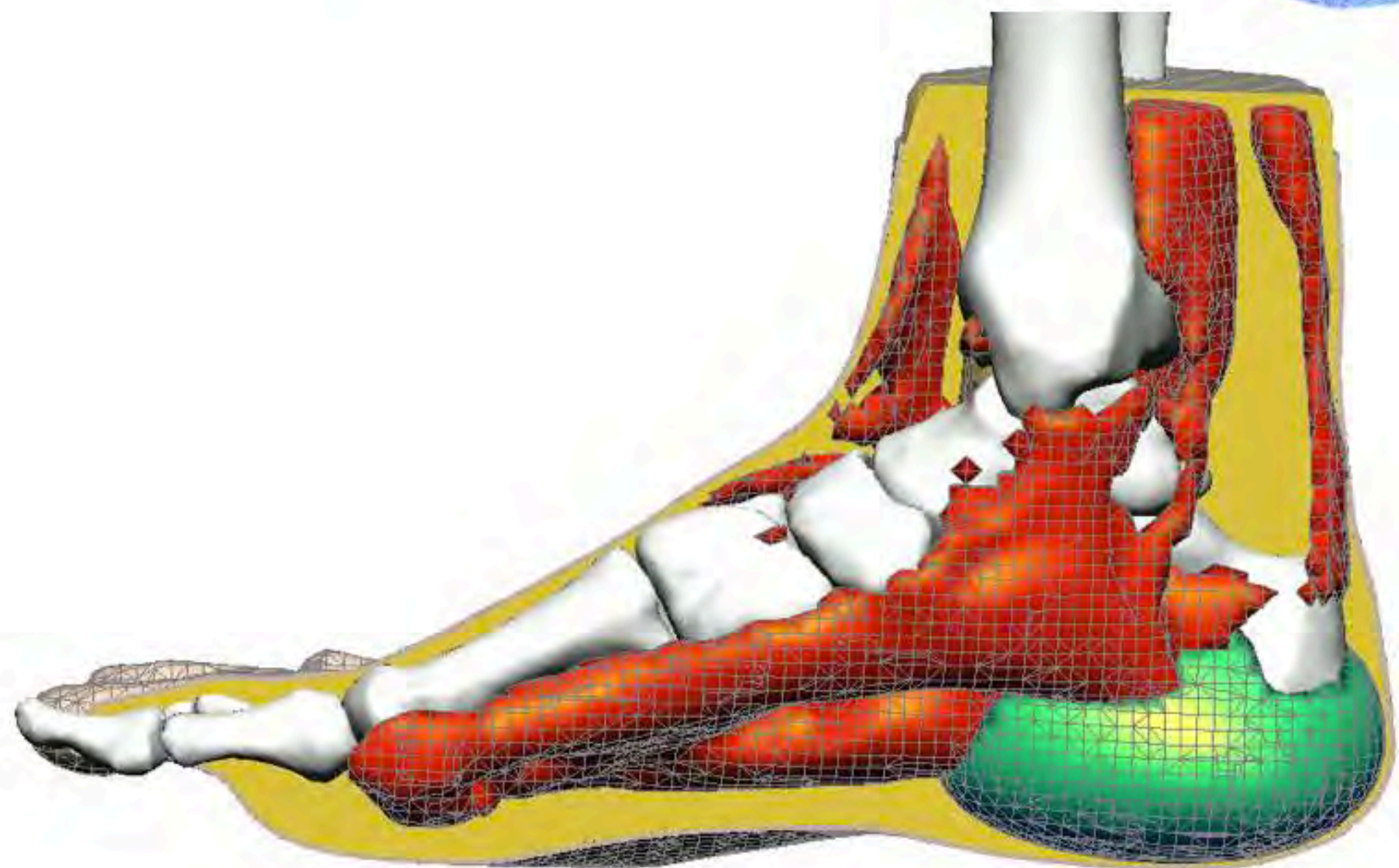
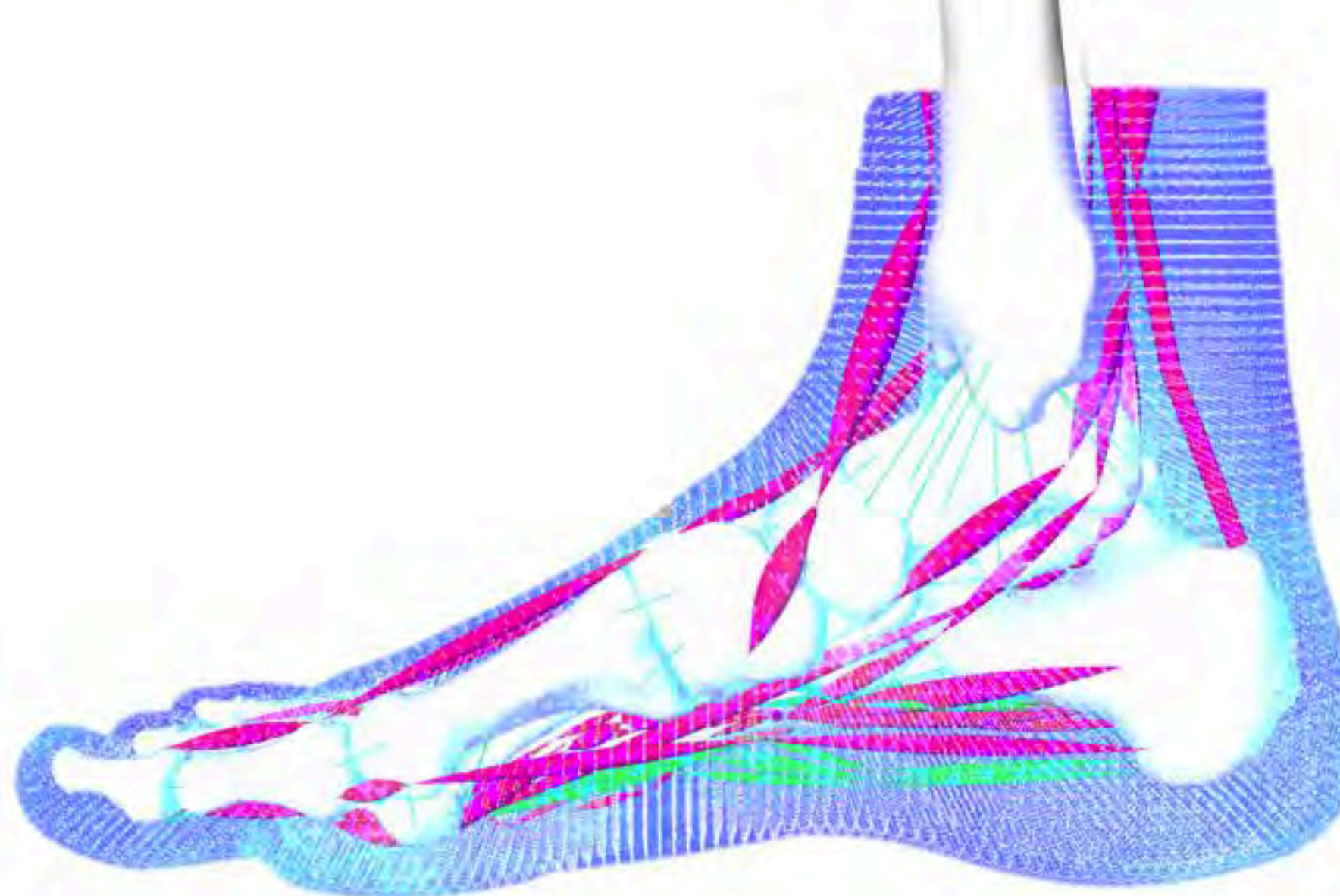
Fat tissue

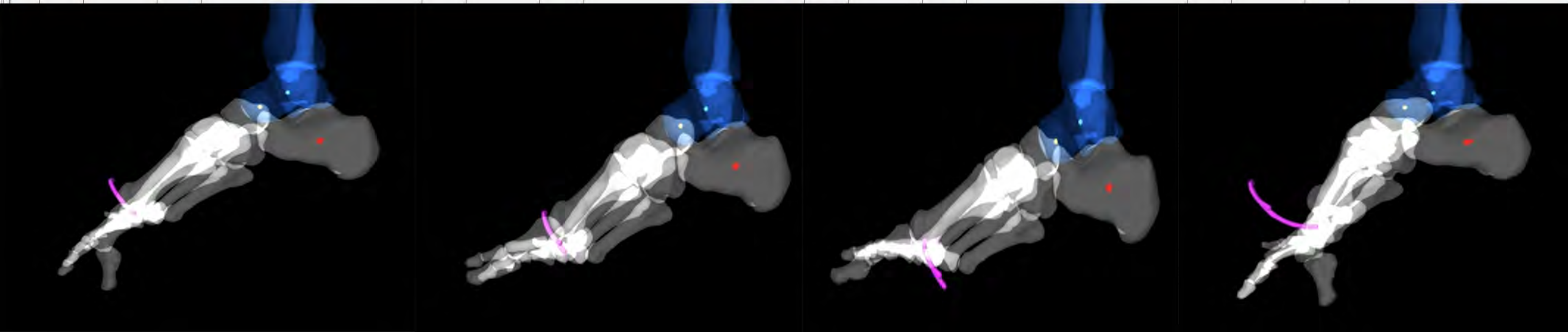
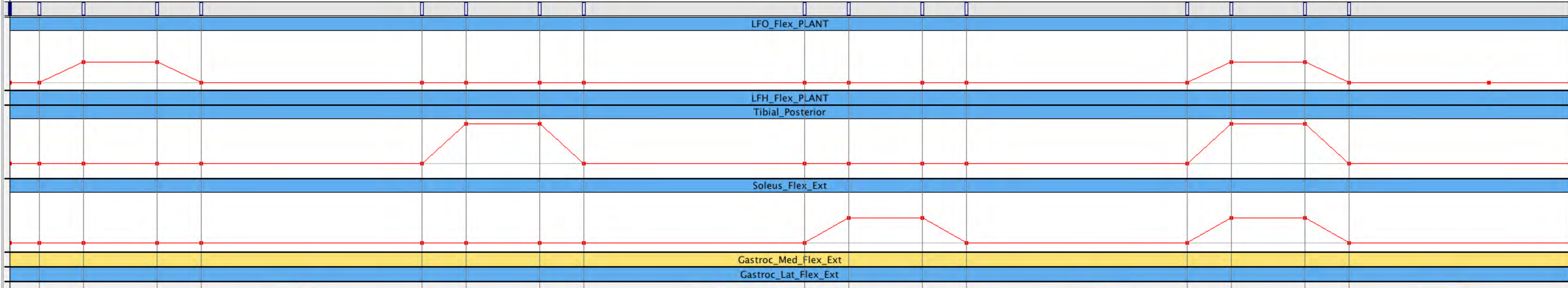


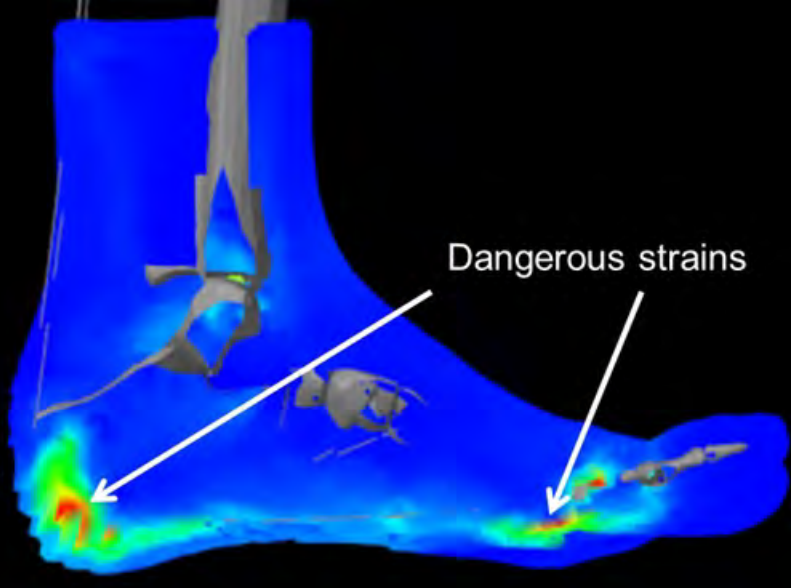
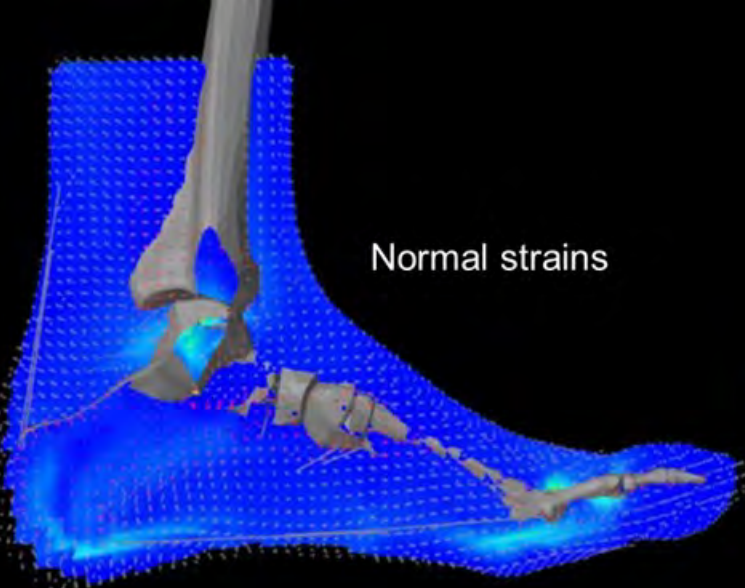
Muscles tissue



Heel Pad







Reference	Team	Year	Application	Constitutive law	Material parameters
Wright et al.		1964		Lig : Li, El, Is	E_Fascia = 260MPa, Nu_fasci=0.4, CS =290.7mm2
Nakamura et al.		1981	Orthosis	Bone: Ho, Is, Li, SoftTis : Ho, Is, NoLi, El	Nu_Bone = 0.3, E_Bone = 7,3GPa, Nu_SoftTis = 0.49 , E_SoftTis= 10MPa
Sieger et al.		1988		Lig : Li, El, Is	E_Lig = 260MPa et Nu_Lig = 0.4, CS=18.4mm2
Schreppers et al.		1990		Meniscus : Li, Ho, Is	E_Bone= 500MPa, Nu_Bone= 0.2, E_cart =10MPa, Nu_cart =0.4, E_menisc= 20MPa et Nu_menisc=0.3
Lemmon et al.	Cavanagh	1997	Orthosis	Bone : Li, SoftTis : HyEl, MoRi	Nu_Bone = 0.34, E_Bone = 10GPa, SoftTis : C10 = 85,550N.m-2, C01 = -58,400, C20= 38,920, C11= -23,100, C02 = 8,484, D1 = 0.4370E-05, D2 = 0.6811E-06
Athanasίου et al.	1998	1998		Bone: Nakamura 1981. Cart : li, is, El	Bone: Nakamura 1981, E_cart=1.01MPa, Nu_Cart= 0.4
Jacob et al.	Patil	1999	Neuropathy	Bone, Cart, Lig : Ho, Is, Li, SoftTis : Li	Bone: Nakamura 1981, Cart : Schreppers 1990 , Lig_Stiff = 1,5N/mm, Nu_SoftTis = 0,49, E_SoftTis= 1MPa
Gefen	Gefen	2000	Physiology	Bone : Nakamura 1981. SoftTis: NoLi	Bone : Nakamura 1981 , Cart : Athanasίου 1998 ,Nu_SoftTis= 0.49
Chen et al	Chen	2001	Physiology	Bone et SoftTis : Li, ho, El	Bone : Lemmon 1997, Cart : Schreppers 1990 Nu_SoftTis= 0.49, E_SoftTis= 1.15MPa, E_Lig= 11MPa
Chen et al	Chen	2003	Orthosis	Chen 2001	Bone : lemmon 1997, Cart : Schreppers 1990, SoftTis Chen 2001
Gefen	Gefen	2003	Diabetes	Bone : Nakamura 1981 , SoftTis: Gefen 2000	Bone : Nakamura 1981 , SoftTis: Gefen 2000
Thomas et al.	Patil	2004	Diabetes	Bone : Nakamura 1981, Cart : Schreppers 1990, Lig_stif: Patil 1996, SoftTis: Nakamura 1981	Bone : Nakamura 1981, Cart : Schreppers 1990, Lig_stif:Patil 1996, SoftTis: Nakamura 1981
Erdemir et al.	Cavanagh	2005	Orthosis	Bone : Rigid, SoftTis: HyEl , Incomp	SoftTis Ogd Mu1 = 14.3kPa e Alpha1 = 7.3
Cheung & Zhang.	Zhang	2005	Orthosis	Bone : Nakamura 1981, Cart : Schreppers 1990, Lig : Ho, Isn li, SoftTis: MoRi, HyEl, Is	Bone : Nakamura 1981, Cart: Athanasίου 1998, Lig : Sieger 1988, Fascia : Wright 1964, E_SoftTis= 450KPa, Nu_SoftTis= 0,49
Actis et al.	Actis	2006	Diabetes	Bone: Nakamura, Cart, tendon fasci : Li El; SoftTis: NoLi	E_SoftTis = 0.30MPa, C= 60MPa-1, Nu_SoftTis= 0.45, E_Fascia= 85MPa, E_tendon=15MPa
GBoneke et al.	Cavanagh	2006	Orthosis	Bone et SoftTis : Erdemir 2005, Heelpad : HyEl,Incomp	Bone et SoftTis : Erdemir 2005, Heel pad: Mu1=16.45 kPa, Alpha = 6.82
Erdemir et al	Cavanagh	2006	Diabetes	Bone et SoftTis : Erdemir 2005; Heel pad: GBoneke 2006	Bone et SoftTis : Erdemir 2005; Heel pad: GBoneke 2006
Cheung et al.	Zhang	2006	Diabetes	Bone: Nakamura 1981, Cart : Schreppers1990, SoftTis : Lemmon 1997	Bone: Nakamura 1981, Cart : Schreppers1990, SoftTis : Lemmon 1997, Lig : Sieger 1988, Fascia : Wright 1964

Antunes et al.		2006	Physiology	Bone: Nakamura 1981, Cart : Schreppers1990, SoftTis : Lemmon 1997, Lig : Sieger 1988, Fascia : Wright 1964	Bone: Nakamura 1981, Cart : Schreppers1990, SoftTis : Lemmon 1997, Lig : Sieger 1988, Fascia : Wright 1964
Budhabhatti et al.	Cavanagh	2007	Orthopedy	Bone et SoftTis : Erdemir 2005; Heel pad: GBoneke 2006	Bone et SoftTis : Erdemir 2005; Heel pad: GBoneke 2006
Actis et al.	Actis	2008	Orthesis	Bone: Nakamura, Cart, tendon fasci : Li El; SoftTis: Noli	E_SoftTis = 0.30MPa, C= 60MPa-1, Nu_SoftTis= 0.45, E_Fascia= 85MPa, E_tendon=15MPa
Cheung et Zhang	Zhang	2008	Diabetes	Bone: Nakamura 1981, Cart : Schreppers1990, SoftTis : Lemmon 1997, Lig : Sieger 1988, Fascia : Wright 1964	Bone: Nakamura 1981, Cart : Schreppers1990, SoftTis : Lemmon 1997, Lig : Sieger 1988, Fascia : Wright 1964
Agic et al.,		2008	Diabetes	Bone: Nakamura 1981, Cart : Schreppers1990, SoftTis : Lemmon 1997, Lig : Sieger 1988, Fascia : Wright 1964	Bone: Nakamura 1981, Cart : Schreppers1990, SoftTis : Lemmon 1997, Lig : Sieger 1988, Fascia : Wright 1964
Garcia-Aznar et al.	Bayod	2009	Orthopedy	Bone: Ho, li,El,Is	E_Bone_Cortical=17GPa E_Bone_Trabeculaire= 700MPa, Nu_Bone=0.3 Cart:Scheppers 1990, Lig et Fascia = Cheung 2005.
Garcia-Gonzalez et al	Bayod	2009	Orthopedy	Bone cortical et trabecular: Garcia 2009, Cart : Scheppers 1990, Lig : Sieger 1988, Fascia : Wright 1964	Bone cortical et trabecular: Garcia 2009, Cart : Scheppers 1990, Lig : Sieger 1988, Fascia : Wright 1964
Shariatmadari et al.		2009	Diabetes	Bone : Nakamura 1981, SoftTis : Erdemir 2005	Bone : Nakamura 1981, SoftTis : Erdemir 2005
Bayod et al.	Bayod	2010	Orthopedy	Bone: Garcia 2009, Cart : Schreppers 1990, Lig et Fasca : Cheung 2005 et Tendons: Li, El, Incomp	Bone: Garcia 2009, Cart : Schreppers 1990, Lig et Fasca : Cheung 2005 et E_Tend=450MPa, Nu_Tend=0.3 , CS= 12.5mm2
Halloran et al.	Cavanagh	2010	Physiology	Bone : Nakamura 1981, SoftTis : Erdemir 2005	Bone : Nakamura 1981, SoftTis : Erdemir 2005
Chen et al.	Chen WM	2010	Physiologie	Bone: Nakamura 1981, Cart : Athanasiou 1998, Lig : Sieger 1988, Fascia : Wright 1964; SoftTis = Lemmon 1997	Bone: Nakamura 1981, Cart : Athanasiou 1998, Lig : Sieger 1988, Fascia : Wright 1964; SoftTis = Lemmon 1997
Tao et al.	Tao	2010	Physiology	Bone: Nakamura 1981, Cart : Athanasiou 1998, Lig : Sieger 1988, Fascia : Wright 1964; SoftTis = Cheung 2005	Bone: Nakamura 1981, Cart : Athanasiou 1998, Lig : Sieger 1988, Fascia : Wright 1964; SoftTis = Cheung 2005
Gu et al	Gu	2010	Diabetes	Bone: Nakamura 1981, Cart : Athanasiou 1998, Lig : Sieger 1988, Fascia : Wright 1964; SoftTis = Lemmon 1997	Bone: Nakamura 1981, Cart : Athanasiou 1998, Lig : Sieger 1988, Fascia : Wright 1964; SoftTis = Lemmon 1997
Gu et al	Gu	2010	Physiologie	Bone: Nakamura 1981, Cart : Athanasiou 1998, Lig : Sieger 1988, Fascia : Wright 1964; SoftTis = Lemmon 1997	Bone: Nakamura 1981, Cart : Athanasiou 1998, Lig : Sieger 1988, Fascia : Wright 1964; SoftTis = Lemmon 1997

Sopher et al.	Gefen	2011	Diabetes	Bone : Nakamura 1981, SoftTis : Ogd;	Mu_Skin= 640kPa, Mu_fat=0.29kPa, Alpha_skin= 6.8 Alpha_fat= 8.8 ,K_Skin= 63.8MPa, k_fat=28.9kPa
Gu et al	Gu	2011	Physiology	Bone: Nakamura 1981, Cart : Athanasiou 1998, Lig : Sieger 1988, Fascia : Wright 1964; SoftTis = Lemmon 1997	Bone: Nakamura 1981, Cart : Athanasiou 1998, Lig : Sieger 1988, Fascia : Wright 1964; SoftTis = Lemmon 1997
Liang et al.		2011	Physiology	Bone: Nakamura 1981, Cart : Athanasiou 1998, Lig : Sieger 1988, Fascia : Wright 1964;	Bone: Nakamura 1981, Cart : Athanasiou 1998, Lig : Sieger 1988, Fascia : Wright 1964;
Luo et al.		2011	Diabetes	SoftTis: NoLi, HyEl, Ogden	Mu1=-0.680724MPa, Alpha1=-0.62956,Mu2= 0.656916MPa, alpha2=-0.41635
Bayod et al.	Bayod	2012	Orthopedy	Bone cortical et trabecular: Garcia 2009, Cart : Scheppers 1990, Lig : Sieger 1988, Fascia : Wright 1964	Bone cortical et trabecular: Garcia 2009, Cart : Scheppers 1990, Lig : Sieger 1988, Fascia : Wright 1964
Sun et al.	Chen	2012	Physiology	Bone: Nakamura 1981, Cart : Athanasiou 1998, Lig : Sieger 1988, Fascia : Wright 1964; SoftTis = Cheung 2005	Bone: Nakamura 1981, Cart : Athanasiou 1998, Lig : Sieger 1988, Fascia : Wright 1964; SoftTis = Cheung 2005
Chen et al.	Chen	2012	Diabetes	Bone: Nakamura 1981, Cart : Athanasiou 1998, Lig : Sieger 1988, Fascia : Wright 1964; SoftTis = Lemmon 1997	Bone: Nakamura 1981, Cart : Athanasiou 1998, Lig : Sieger 1988, Fascia : Wright 1964; SoftTis = Lemmon 1997
Xu et al	Zhang	2012	Orthopedy	Bone: Nakamura 1981, Cart : Athanasiou 1998, Lig : Sieger 1988,	Bone: Nakamura 1981, Cart : Athanasiou 1998, Lig : Sieger 1988,
Spyrou and Aravas		2012	Physiology	Bone: Nakamura 1981, Cart : Athanasiou 1998, Lig : Sieger 1988, Fascia : Wright 1964; SoftTis = Lemmon 1997	Bone: Nakamura 1981, Cart : Athanasiou 1998, Lig : Sieger 1988, Fascia : Wright 1964; SoftTis = Lemmon 1997
Ozen et al.		2013	Orthopedy	Bone: Nakamura 1981, Cart : Schreppers1990, SoftTis : Lemmon 1997, Lig : Sieger 1988, Fascia : Wright 1964	Bone: Nakamura 1981, Cart : Schreppers1990, SoftTis : Lemmon 1997, Lig : Sieger 1988, Fascia : Wright 1964
Wang	Zhang	2014	Orthopedy	Bone: Nakamura 1981, Cart : Athanasiou 1998, Lig : Sieger 1988, Fascia : Wright 1964; SoftTis = Cheung 2005	Bone: Nakamura 1981, Cart : Athanasiou 1998, Lig : Sieger 1988, Fascia : Wright 1964; SoftTis = Cheung 2005
WONG	Zhang	2014	Orthopedy	Bone: Nakamura 1981, Cart : Athanasiou 1998, Lig : Sieger 1988, Fascia : Wright 1964; SoftTis = Cheung 2005	Bone: Nakamura 1981, Cart : Athanasiou 1998, Lig : Sieger 1988, Fascia : Wright 1964; SoftTis = Cheung 2005
LuSoz et al	Payan	2015	Diabetes	Bone: rigid, Soft tissues : Neo Hook inspired by Sopher et al. 2011	Bone: rigid, Soft tissues: skin (200 kPa, 0.495), fat (30 kPa, 0.49) tendon (1 Gpa, 0.495), and muscles (60 kPa, 0.495)
Chen et al	Chen	2015	Orthesis	Bone: Nakamura 1981, Cart : Athanasiou 1998, Lig : Sieger 1988, Fascia : Wright 1964; SoftTis = Cheung 2005	Bone: Nakamura 1981, Cart : Athanasiou 1998, Lig : Sieger 1988, Fascia : Wright 1964; SoftTis = Cheung 2005